



ELSEVIER

Contents lists available at ScienceDirect

Measurement

journal homepage: www.elsevier.com/locate/measurement

Experimental evaluation of accuracy and repeatability of a novel body-to-sensor calibration procedure for inertial sensor-based gait analysis



Eduardo Palermo^{a,b,*}, Stefano Rossi^{b,c}, Francesca Marini^d, Fabrizio Patanè^{a,b}, Paolo Cappa^{a,b}

^a Department of Mechanical and Aerospace Engineering, "Sapienza" University of Rome, Via Eudossiana, 18, 00184 Rome, Italy

^b Movement Analysis and Robotics Laboratory (MARLab), Neurorehabilitation Division, IRCCS Children's Hospital "Bambino Gesù", Via Torre di Palidoro, 00050 Passoscuro, Fiumicino, Rome, Italy

^c Department of Economics and Management – Industrial Engineering, University of Tuscia, Via del Paradiso, 47, 01100 Viterbo, Italy

^d Robotics Brain and Cognitive Science Department, Italian Institute of Technology (IIT), Genoa, Italy

ARTICLE INFO

Article history:

Received 5 September 2013

Received in revised form 29 January 2014

Accepted 6 March 2014

Available online 18 March 2014

Keywords:

IMU/MIMU

Inertial sensors

Gait analysis

Anatomical calibration

Joint angular kinematics

ABSTRACT

This paper describes a novel functional body-to-sensor calibration procedure for inertial sensor-based gait analysis. The procedure is designed to be easily and autonomously performable by the subject, without the need for precise sensor positioning, or the performance of specific movements. The procedure consists in measuring the vertical axis during two static positions, and is not affected by magnetic field distortion. The procedure has been validated on ten healthy subjects using an optoelectronic system to measure the actual body-to-sensor rotation matrices.

The effects of different sensor positions on each body segment, or different levels of subject inclination during the second static position of the procedure, resulted unnoticeable. The procedure showed accuracy and repeatability values less than 4° for each angle except for the ankle int-external rotation (9.7°, 7.2°). The results demonstrate the validity of the procedure, since they are comparable with those reported for the most-adopted protocols in gait analysis.

© 2014 Elsevier Ltd. All rights reserved.

1. Introduction

The recent technological advances in MEMS caused a renewed interest in the use of Inertial Measurement Units (IMUs) to perform effective biomechanical studies such as fall detection, gesture recognition, and locomotion analysis in healthy subjects and in patients with pathology [1–9]. IMUs are generally referred to as a combination of linear accelerometers and gyroscopes – from a minimal setup to measure 3D motion to redundant setups [10–12] – and

when the cluster also includes magnetometers, they are referred as MIMUs. From the comparative examination of IMU/MIMUs with optoelectronic systems (OSs), which are considered the golden standard for human motion analysis, it emerges that the IMU/MIMUs have the following general advantages: they do not require a dedicated laboratory, they permit a wider workspace, and they are low cost devices [13]. Their main drawbacks are as follows. Firstly, IMU/MIMUs are affected by intrinsic bias and inaccuracy due to the drift related to the integration of gyroscope data; actually, this produces large inaccuracy in the estimation of angular rotations and still greater effects in the evaluation of linear velocities and displacements [14,15]. Secondly, MIMUs are prone to disturbance effects induced by the presence of ferromagnetic materials around

* Corresponding author at: Department of Mechanical and Aerospace Engineering, "Sapienza" University of Rome, Via Eudossiana, 18, 00184 Rome, Italy. Tel.: +39 06 44585585.

E-mail address: eduardo.palermo@uniroma1.it (E. Palermo).

the sensors [16–20]. Nevertheless, the main strength of IMU/MIMUs is represented by data fusion algorithms, designed to reduce these errors under values acceptable for human motion analysis. So far several algorithms have been proposed [15,19,21–24].

An additional issue related to IMU/MIMU-based systems in the study of human motion is the alignment of sensor axes with anatomical ones. In fact, due to their inaccessibility, the problem is solved performing a calibration procedure for the assessment of the relative rotation between sensor and body segment frames. Picerno et al. [25] proposed an *ad hoc* tool instrumented with a MIMU, nominally identical to the sensors placed on the subject, for the evaluation of the body-to-sensor rotation matrices for the lower limb. The tool was designed to touch some anatomical landmarks, while the sensor placed on the tool measured the orientation of the vector connecting the landmarks expressed in its reference frame. This intermediate step led to the computation of each body-to-sensor matrix, under the assumption that both the pointer MIMU and the one placed on the body segment had the same reference frame.

From a survey of the literature, it emerges that most of the calibration procedures proposed were based on a functional approach for the kinematic evaluation of upper [26,27] and lower limbs [28,29]. In the functional approach, the estimation of anatomical axes is carried-out measuring the components of the gravity acceleration vector in predefined segment orientations, and/or the components of the angular velocity vector between two consecutive body segments during joint rotations, often performed with the help of an operator. The mentioned vectors measured in the sensor frame were assumed to be parallel to the anatomical axes during static positions or movements. Focusing on lower limb analysis, O'Donovan et al. [28] defined a two-phase functional calibration procedure. Anatomical axes, for ankle kinematics evaluation, were estimated in the sensor frame during two body segment rotations: the first around the longitudinal axis of tibia and the second around the knee flexion axis. However, accurately performing a whole-body rotation while maintaining the longitudinal axis of tibia parallel to the vertical axis may be difficult, especially for patients. In order to perform the knee kinematics evaluation, in fact, Favre et al. [29] let an examiner move the shank of the subject during the calibration procedure to estimate anatomical axes of tibia in the corresponding sensor frame. Cutti et al. [30,31], introduced the “Outwalk” protocol for MIMU sensors placement and a functional calibration procedure, in order to make fast and comfortable the use of MIMUs for joint kinematics evaluation. The protocol is the most complete in terms of segments involved and procedure description, as well as the easiest to perform. It provides indications for MIMU positioning and anatomical frame definition of 7 segments modeled lower limb plus thorax, during standing position, and a knee flexion movement to compute the mean knee flexion–extension axis. However, the protocol requires a precise positioning for some sensors, positioned at the pelvis, thorax or shank. The effects of mounting the sensors with a slightly different orientation or position may cause a further degradation

of experimental data with an increase of standard deviation both in retesting the same subject and in examining different individuals.

The previously mentioned calibration procedures require: (i) the presence of an expert operator to help the subject in performing specific movements or to mount MIMUs in well-defined positions; or, finally, (ii) to handle additional tools. These requirements actually restrict the use of IMU/MIMU in day-to-day life. Instead, the independent use of the procedure by the subject represents a relevant feature in the context of motion analysis sessions conducted outside of a clinical environment and during daily activity as also reported by previous studies [32–34]. In addition, most of the proposed calibration procedures described above allow the computation of the calibration matrix of a sensor by means of data provided by one or more sensors placed on other body segments. According to Picerno et al. [35], due to local magnetic field distortions, sensor data may be referred not to the same ground frame, compromising the reliability of joint kinematics. Thus, calibration procedures that allow the computation of the body-to-sensor rotation matrix for each sensor independently should be preferred.

It is also worth noting that none of the proposed procedures used the anatomical frame definition introduced by Wu et al. [36], generally accepted as a standard in biomechanics. Actually, the assessment of the orientation of axes defined in their work is not feasible with a functional procedure. This represents a relevant limitation in comparing results of motion analyses conducted via IMU/MIMU and OS.

Taking into account the previously mentioned findings, the aim of the present work is the proposal of a novel two-phase functional calibration procedure for lower-limb kinematics evaluation, designed to obtain the body-to-sensor alignment independently for each sensor and without requiring a skilled experimenter. Then, we intend to evaluate the accuracy and the repeatability of the proposed calibration procedure performed with a commercially available MIMU system relative to the calibration obtained using an OS. In particular, we plan to investigate whether the effects of the calibration repeatability on the measurement of hip, knee and ankle angles during gait were acceptable by gait analysis practices. Additionally, we intend to evaluate the difference between the joint kinematics obtained with the anatomical axes definition introduced for the calibration, and the one obtained with the standard Joint Coordinate System (JCS) definition proposed by Wu et al. [36] and adopted by International Society of Biomechanics (ISB).

2. Material and methods

2.1. Lower-limb joint kinematics

The estimation of joint angles consists in the evaluation of joint rotations between two body segments and, therefore, in the calculation of joint rotation matrices. The rotation matrix ${}^b_i\mathbf{R}_{b_j}$ between two coordinate systems (CS_{b_i} and CS_{b_j}) relative to the body frames b_i and b_j can be computed as follows:

$${}^b_i\mathbf{R}_{b_j} = ({}^g\mathbf{R}_{b_i})^T {}^g\mathbf{R}_{b_j} \quad (1)$$

where the CS_g is the ground fixed coordinate system. Introducing the coordinate systems CS_{s_i} , associated to the i -th sensor, we obtain:

$${}^g\mathbf{R}_{b_i} = {}^g\mathbf{R}_{s_i} {}^s_i\mathbf{R}_{b_i} \quad (2)$$

where ${}^g\mathbf{R}_{s_i}$ represents the output of the i -th inertial sensor placed on the i -th body segment and ${}^s_i\mathbf{R}_{b_i}$ is the related body-to-sensor rotation matrix. The rotation matrix of the joint between i -th and j -th body segment is, therefore, equal to:

$${}^b_i\mathbf{R}_{b_j} = ({}^g\mathbf{R}_{s_i} {}^s_i\mathbf{R}_{b_i})^T {}^g\mathbf{R}_{s_j} {}^s_j\mathbf{R}_{b_j} \quad (3)$$

The ${}^s_i\mathbf{R}_{b_i}$ matrix depends on the biomechanical convention chosen to define the CS_{b_i} . In our work, CS_{b_i} is defined, while the subject is in standing position, as following: z_{b_i} axis coincident with the vertical one z_g and the plane yz_{b_i} parallel to the sagittal plane with y_{b_i} pointing forward. This coordinate system is not an anatomical frame, as the one defined by ISB recommendations, but a technical frame also referred to in the following as TF. TF can be evaluated by means of both MIMUs (TF_MIMU) and an optoelectronic system (TF_OS), which represents the reference technical frame.

2.2. Evaluation of TF_MIMU – functional calibration procedure

The TF_MIMU can be evaluated by means of a functional calibration procedure (FC) that consists in the gathering of the sensor outputs for five seconds with the subject keeping still during two consecutive phases (Fig. 1). Phase A, addressed as FC(A), is conducted while the subject is in a standing upright posture. Phase B, addressed as FC(B), can be carried out while the subject is in a sitting position with the trunk backwards inclined and the legs stretched, addressed as FC(B)-C, or alternatively, while the subject is lying on a table, addressed as FC(B)-T. We proposed the two alternatives for phase B to permit the FC conduction for patients with different pathology severity. We also hypothesize that irrelevant differences in the body-to-sensor rotation estimation are obtained by the combination of FC(A) & FC(B)-C or FC(A) & FC(B)-T. The subject was asked only to maintain the sagittal planes of each body segment parallel between FC(A) and FC(B), avoiding rotations of body segments in frontal and transverse planes. In order to make the procedure easy to be performed by the subject autonomously, we decided to avoid the use of additional tools and/or procedures devoted to limit rotations of body segments in frontal and transverse planes, despite it represents a possible source of uncertainty in the evaluation of body-to-sensor rotation matrices. Thus, one of the aims of this study is the evaluation of accuracy and repeatability of the procedure, including also the above mentioned source of uncertainty.

In FC(A) the z -axis ${}^s_i\mathbf{z}_{b_i}^{MIMU}$ of i -th body frame is defined parallel to the vertical axis z_g , which is coincident to z_{g_i} measured by the MIMU sensor in the local frame:

$${}^s_i\mathbf{z}_{b_i}^{MIMU} = {}^s_i\mathbf{z}_{g_i}^{MIMU_A} \quad (4)$$

In FC(B), the sagittal plane (yz -plane) is defined parallel to ${}^s_i\mathbf{z}_{b_i}^{MIMU}$ and z_{g_i} , with y_{b_i} pointing forward, which is again measured by the MIMU sensor locally:

$${}^s_i\mathbf{x}_{b_i}^{MIMU} = \frac{{}^s_i\mathbf{z}_{b_i}^{MIMU} \times {}^s_i\mathbf{z}_{g_i}^{MIMU_B}}{|{}^s_i\mathbf{z}_{b_i}^{MIMU} \times {}^s_i\mathbf{z}_{g_i}^{MIMU_B}|}, \quad {}^s_i\mathbf{y}_{b_i}^{MIMU} = {}^s_i\mathbf{z}_{b_i}^{MIMU} \times {}^s_i\mathbf{x}_{b_i}^{MIMU} \quad (5)$$

Finally, the rotation matrix ${}^s_i\mathbf{R}_{b_i}^{MIMU}$ is obtained grouping the three unit vectors:

$${}^s_i\mathbf{R}_{b_i}^{MIMU} = \begin{bmatrix} {}^s_i\mathbf{x}_{b_i}^{MIMU} & {}^s_i\mathbf{y}_{b_i}^{MIMU} & {}^s_i\mathbf{z}_{b_i}^{MIMU} \end{bmatrix} \quad (6)$$

We point out that the FC permits calculating ${}^s_i\mathbf{R}_{b_i}^{MIMU}$ using ${}^s_i\mathbf{z}_{g_i}^{MIMU_A}$ and ${}^s_i\mathbf{z}_{g_i}^{MIMU_B}$, which are computed only by means of the accelerometer signals and not by the magnetometer sensor. The procedure is, therefore, inherently unaffected by soft-iron and hard-iron disturbances. Moreover, it is worth noting that, during FC(B), a precise inclination angle in the sagittal plane is not required for each body segment.

2.3. Evaluation of TF_OS

${}^s_i\mathbf{R}_{b_i}^{OS}$ represents the actual relative body-to-sensor matrix measured by means of OS and related to the technical frame. It can be evaluated as:

$${}^s_i\mathbf{R}_{b_i}^{OS} = ({}^g\mathbf{R}_{s_i}^{OS})^T {}^g\mathbf{R}_{b_i}^{OS} \quad (7)$$

where ${}^g\mathbf{R}_{s_i}^{OS}$ represents the rotation matrix between each sensor and the ground reference frame. It can be evaluated by positioning at least three markers on each MIMU. Moreover, ${}^g\mathbf{R}_{b_i}^{OS}$ represents the rotation matrix between each body segment and the ground reference frame and is defined by the ${}^g\mathbf{z}_{b_i}^{OS}$ axis coincident with the vertical one:

$${}^g\mathbf{z}_{b_i}^{OS} = [0 \ 0 \ 1]'$$

For pelvis, thigh and shank, plane xz_{b_i} is defined parallel to the frontal plane:

$${}^g\mathbf{y}_{b_i}^{OS} = \frac{{}^g\mathbf{z}_{b_i}^{OS} \times {}^g\mathbf{p}_{b_i}^{OS}}{|{}^g\mathbf{z}_{b_i}^{OS} \times {}^g\mathbf{p}_{b_i}^{OS}|}, \quad {}^g\mathbf{x}_{b_i}^{OS} = {}^g\mathbf{y}_{b_i}^{OS} \times {}^g\mathbf{z}_{b_i}^{OS} \quad (9)$$

where ${}^g\mathbf{p}_{b_i}^{OS}$ represents the generic vector connecting two anatomical landmarks as described in Table 1.

For the foot, plane yz_{b_i} is defined parallel to the sagittal plane:

$${}^g\mathbf{x}_{b_i}^{OS} = \frac{{}^g\mathbf{p}_{b_i}^{OS} \times {}^g\mathbf{z}_{b_i}^{OS}}{|{}^g\mathbf{p}_{b_i}^{OS} \times {}^g\mathbf{z}_{b_i}^{OS}|}, \quad {}^g\mathbf{y}_{b_i}^{OS} = {}^g\mathbf{z}_{b_i}^{OS} \times {}^g\mathbf{x}_{b_i}^{OS} \quad (10)$$

Finally, for each body segment, the rotation matrix ${}^g\mathbf{R}_{b_i}^{OS}$ is obtained grouping the three unit vectors:

$${}^g\mathbf{R}_{b_i}^{OS} = \begin{bmatrix} {}^g\mathbf{x}_{b_i}^{OS} & {}^g\mathbf{y}_{b_i}^{OS} & {}^g\mathbf{z}_{b_i}^{OS} \end{bmatrix} \quad (11)$$

TF_OS is evaluated when the subject is in standing position which, therefore, is coincident with FC(A) of TF_MIMU.

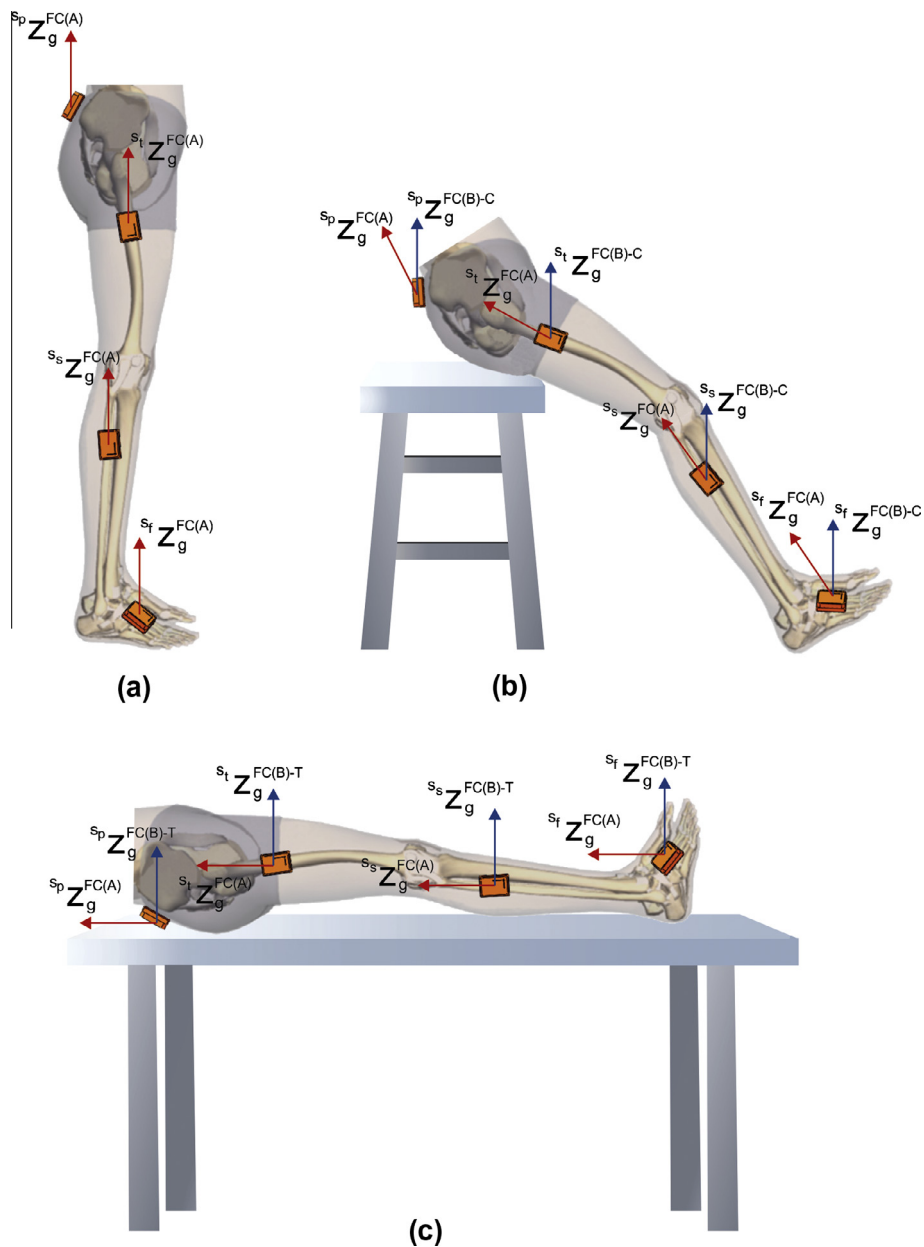


Fig. 1. Functional calibration procedure, FC. Vertical axis gathered in: (a) standing upright posture, FC(A); (b) sitting position with the trunk backwards inclined and the legs stretched, FC(B)-C; and (c) lying on a table, FC(B)-T.

Table 1

Vector ${}^s p_{bi}^{OS}$ definition basing on anatomical landmarks.

Body segment	Vector ${}^s p_{bi}^{OS}$	
	Origin	End point
Pelvis	Left anterior superior iliac spine (LASI)	Right anterior superior iliac spine (RAS)
Thigh	Estimated knee joint center (R/LFEO)	Lateral epicondyle of the knee (R/LKNEE)
Shank	Estimated knee joint center (R/LTIO)	Lateral malleolus (R/LTIB)
Foot	Calcaneus (R/LHEE)	Second metatarsal head (R/LTOE)

2.4. Experimental set-up

Ten healthy subjects (mean age 25 ± 2 years) were enrolled in the study. All volunteers gave informed consent for participation in the experiment. Each subject was instrumented with 7 MIMUs (MTws Xsens Technologies, Enschede, The Netherlands), placed on pelvis and thigh, shank and foot of both sides by means of click-in body straps. The sampling rate was set at 60 Hz. Before the experimental sessions, the MTws were warmed-up for 20 min and then they were aligned outdoors, at least 3 m away from metallic objects, and their heading output was reset.

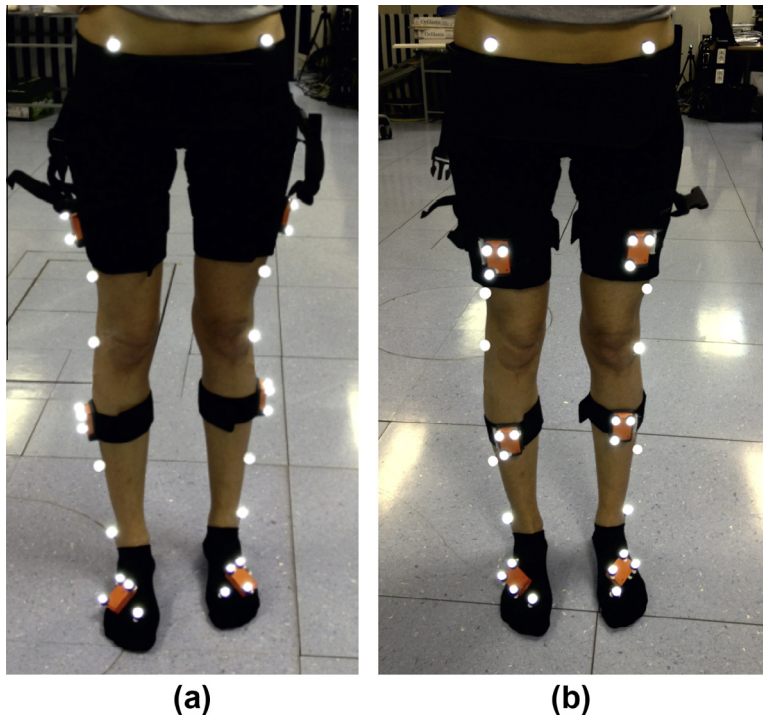


Fig. 2. MIMU positions in: (a) MP-1, and (b) MP-2.

An 8-camera VICON system (MX camera-workstation, Oxford Metrics Group, UK) was used as OS. The sampling rate was set at 200 Hz. Static and dynamic calibration tests, performed in accordance with the manufacturer's indications, showed that the overall RMSE of marker coordinates in three-dimensional space was about 1 mm. Each subject was instrumented with sixteen reflective markers according to the Lower Limb PiG protocol, allowing the computation of anatomical coordinate frames of each body segment [37]. Moreover, three reflective markers were placed on each MIMU in order to acquire its absolute orientation by means of OS. The OS acquired the position of each marker when the subject was in standing position in order to measure TF_OS and the anatomical frame JCS [36]. Finally, the gait kinematics was acquired only by means of MIMUs, because the accuracy of inertial sensors in respect to OS in the evaluation of joint angles is not a subject of this work.

2.5. Experimental procedure

Subjects performed two experimental sessions which differed in the position of MIMUs (MP) on each body segment (we referred to these conditions as MP-1 and MP-2, see Fig. 2) in order to verify whether the FC procedure is affected by a different position/orientation of inertial sensors. During each experimental session, subjects performed the functional calibration procedure in two different ways, changing the inclination of the body in the sagittal plane during phase (B): FC(A) & FC(B)-C and FC(A) & FC(B)-T. The purpose of the two subject positions

is to evaluate, as previously mentioned, whether the FC(B) can be conducted without paying attention on the inclination angles of each body segment in the sagittal plane. In order to evaluate the repeatability of TF_MIMU, the whole FC procedure – FC(A), FC(B)-C and FC(B)-T – was repeated three times. The reference technical frame TF_OS and the anatomical frame ISB were evaluated basing on position of reflective markers acquired during the first repetition of FC(A). Finally, the subjects performed 4 gait analysis trials in order to collect kinematic data from MIMUs in 20 strides. The experimental session is divided into two subsections which differ in sensor position (MP-1 and MP-2). The time sequence of the overall procedure is reported below:

1. Sensor position MP-1 (Fig. 2(a)):
 - 1.a. MIMUs were positioned on the subject in MP-1 configuration.
 - 1.b. Subject performed three repetitions of FC(B)-C and three repetitions of FC(B)-T; during each repetition output of the MIMUs was acquired for five seconds.
 - 1.c. Reflective markers were placed on subject and on MIMUs.
 - 1.d. Subject performed three repetitions of FC(A) (five seconds each); OS captured marker positions only during the first repetition.
 - 1.e. Subject performed walking trials, acquired only by means of MIMUs.
2. Sensor position MP-2 (Fig. 2(b)):
 - 2.a. MIMUs were shifted to MP-2 position, without removing markers.

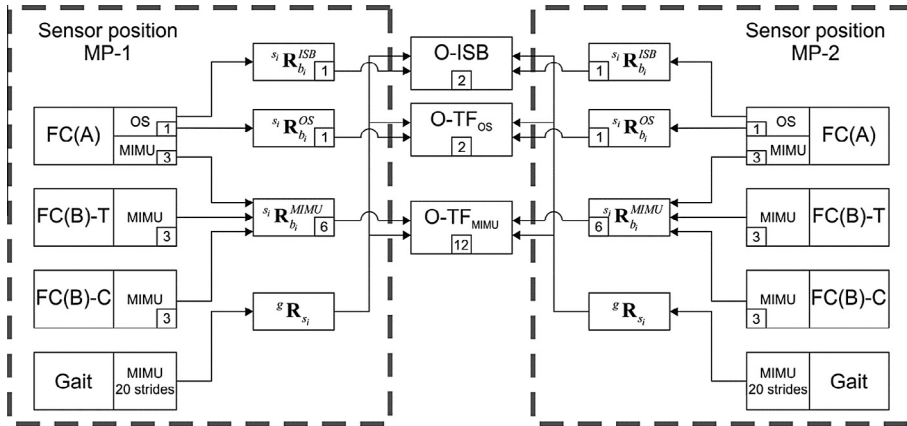


Fig. 3. Scheme of the data processing procedure. O-ISB and O-TF_{OS} contains 2 curves per joint angle, deriving from trials conducted in MP-1 and MP-2 condition. O-TF_{MIMU}, instead contains 12 curves per joint angle (3 repetitions for both FC(B)-C and FC(B)-T).

- 2.b. Subject performed three repetitions of FC(A) (five seconds each); OS captured marker positions only during the first repetition.
- 2.c. Subject performed walking trials, acquired only by means of MIMUs.
- 2.d. Reflective markers were removed.
- 2.e. Subject performed three repetitions of FC(B)-C and three of FC(B)-T (five seconds each).

As observable, the time sequence after sensor shifting in MP-2 position is composed by the same activities performed in MP-1 condition, but in a different order. This choice has been made only to avoid the repetition of marker positioning procedure, which could be affected by measurement repeatability. In post processing phase the processing order of computations described in section for FC procedure has been restored.

2.6. Data processing

Fig. 3 represents a scheme of the data processing procedure. As reported in (2), the time varying rotation matrix of each body segment ${}^g\mathbf{R}_{b_i}$ was obtained knowing matrix ${}^g\mathbf{R}_{s_i}$ during walking trials, and the body-to-sensor matrix ${}^s\mathbf{R}_{b_i}$. Three different ${}^s\mathbf{R}_{b_i}$ were performed to validate the FC procedure. In particular, ${}^s\mathbf{R}_{b_i}^{MIMU}$ and ${}^s\mathbf{R}_{b_i}^{OS}$, which represent the body-to-sensor matrices related to the technical frame, were evaluated by means of the MIMU and OS output following the methodology proposed in Sections 2.2 and 2.3. Moreover, ${}^s\mathbf{R}_{b_i}^{ISB}$, which represents the body-to-sensor rotation matrix related to the standard anatomical frame and obtained following the ISB recommendations [36], was also calculated by means of the OS while the subject was in FC(A). Since the accuracy of inertial sensors is not a topic of this work, we used the same motion tracking data obtained from MIMUs to obtain ${}^g\mathbf{R}_{s_i}$. Subsequently, three joint rotation matrices ${}^b\mathbf{R}_{b_i}$ were evaluated for each couple of consecutive body segments: ${}^b\mathbf{R}_{b_i}^{MIMU}$, ${}^b\mathbf{R}_{b_i}^{OS}$ and ${}^b\mathbf{R}_{b_i}^{CS}$. Therefore, from these joint rotation matrices, the angle curves of each joint related to TF and ISB were obtained in 20 strides and the curves from the different strides have been appended to each other. Finally, we obtained three

output sets referred to as O-TF_{MIMU}, O-TF_{OS} and O-ISB. In particular, for each subject O-TF_{MIMU} includes twelve curves for each joint angle: 3 repetitions x 2 subject positions (i.e., FC(B)-T and FC(B)-C) x 2 MIMU positions (i.e., MP-1 and MP-2). Both O-TF_{OS} and O-ISB, instead, include two curves for each joint angle: one for each MIMU position (i.e., MP-1 and MP-2).

Joint angular curves from O-TF_{MIMU}, O-TF_{OS} and O-ISB have been combined to obtain three main curve similarity indicators: mean absolute variability (MAV), waveform distortion (WD), and the Pearson correlation coefficient (r).

MAV indicator is defined as [31]:

$$MAV = \frac{\sum_{t=0}^T |M(t) - m(t)|}{T} \quad (12)$$

where $M(t)$ and $m(t)$ are respectively:

$$\begin{aligned} M(t) &= \max(y(t)_i, y(t)_{REF}) \\ m(t) &= \min(y(t)_i, y(t)_{REF}) \end{aligned} \quad (13)$$

$y(t)_i$ represents the i -th angle curve reported in O-TF_{MIMU}; $y(t)_{REF}$ represents the i -th reference curve reported in O-TF_{OS} or O-ISB depending on each experimental test that will be described in the following section; T is the total number of frames.

In particular the MAV can be interpreted as an index of the overall uncertainty of the FC procedure. Thus, we referred to mean and standard deviation MAV values as accuracy and repeatability respectively. WD indicator, which represents the intensity of distortion between the i -th angle curve $y(t)_i$ and the reference curve $y(t)_{REF}$, is defined as:

$$WD = \sqrt{\frac{\sum_{t=0}^T (e(t)_i - \bar{e}(t)_i)^2}{T}} \quad (14)$$

where:

$$e(t)_i = y(t)_i - y(t)_{REF} \quad (15)$$

The Pearson coefficient r is evaluated between each $y(t)_i$ and $y(t)_{REF}$. The values of r were interpreted as follows [31]:

- 0.65–0.75: moderate correlation;
- 0.75–0.85: good correlation;

- 0.85–0.95: very good correlation;
- 0.95–1 excellent correlation.

Finally, the joint angle curves considered were the three hip rotations – flex-extension (H_{FE}), ad-abduction (H_{AA}) and int-external rotation (H_{IE}) – the three ankle rotations – dorsi-plantar flexion (A_{DP}), inv-eversion (A_{IV}) and int-external rotation (A_{IE}) – and the knee flexion/extension (K_{FE}), since the knee varus-valgus and internal-external rotation are not considered in the clinical routine due to their low accuracy [38].

2.7. Data analysis

In order to evaluate the repeatability and the accuracy of the FC, we decided to perform three analysis tests, reported below.

2.7.1. Test 1 – influence of MP and subject position in FC(B)

The three above-mentioned indicators were computed between each curve in O-TF_{MIMU} and the corresponding one in O-TF_{OS}. Mean and standard deviation of MAV and WD for MP-1 and MP-2 and for FC(B)-T and FC(B)-C were computed. Then, two-way ANOVA tests were performed to assess whether the FC proposed can be considered independent from subject position in FC(B), that is FC(B)-C and FC(B)-T, and/or MIMU position, that is MP-1 and MP-2.

2.7.2. Test 2 – evaluation of the accuracy and repeatability of FC in respect to a non-anatomical frame (O-TF_{MIMU} vs. O-TF_{OS})

Mean and standard deviation values of MAV and WD were computed between O-TF_{MIMU} and O-TF_{OS} in order to assess the accuracy and precision of the FC. Moreover, the MAV values were compared to the corresponding values reported by Ferrari et al. [39], obtained performing gait analysis trials with five different OS protocols. Minimum values of r have been evaluated to assess the correlation between O-TF_{MIMU} and O-TF_{OS} curves.

2.7.3. Test 3 – evaluation of the accuracy and repeatability of FC in respect to the standard anatomical frame ISB (O-TF_{MIMU} vs. O-ISB)

Similarly to Test 2, the same values were computed between O-TF_{MIMU} and O-ISB in order to assess the influence of a non-anatomical frame definition in the joint angle evaluation.

3. Results and discussion

Fig. 4 shows means (blue lines) and standard deviation areas (pink stripes) of joint angular curves related to a stride for one subject, taking into account each body-to-segment rotation matrix determined with the FC procedure. In Fig. 4 are also depicted the corresponding joint angular curves measured with OS and expressed both in the technical frame TF_OS (black dashed lines) and in the anatomical one JCS (black solid lines).

3.1. Test 1 – influence of MP and subject position in FC(B)

Table 2 reports means and standard deviations for MAV calculated between O-TF_{MIMU} and O-TF_{OS} as a function of subject position and sensor position in FC(B). Differences in sensor position conditions were significant only for K_{FE} and A_{IV} of the left side ($p < 0.01$) and for A_{IV} and A_{IE} of the right side ($p < 0.01$). The MAV index, instead, was significantly different in subject position only for A_{IE} on the right side ($p = 0.03$). These differences can be ascribed to an inaccurate orientation of the foot during FC(B). In fact, the feasibility of the FC procedure is based on the hypothesis that the sagittal plane of each body segment is coincident during the two phases of FC. Keeping the sagittal planes of body segments in FC(B)-C or in FC(B)-T parallel to the same planes when the subject is in FC(A), is more difficult for the foot than for other body segments, due to its higher mobility. Except for A_{IE} in both sides, the reported MAV were always $< 5^\circ$ and the MAV differences between MP-1 and MP-2 were never $> 2.4^\circ$ and between FC(B)-T and FC(B)-C were never $> 1.1^\circ$. Despite variance analysis results, such low difference values imply that different sensor and/or subject positions are *de facto* non influential on the estimation of joint kinematics during gait.

In Table 3 mean and standard deviation values of WD obtained comparing O-TF_{MIMU} and O-TF_{OS} as a function of subject position and sensor position in FC(B) are reported. The WD index was significantly different in sensor position conditions for K_{FE} and A_{DP} on the left side ($p < 0.01$) and for A_{DP} and A_{IV} on the right side ($p < 0.01$). Differences in subject position were significant for A_{DP} and A_{IV} on the left side ($p < 0.01$). WD differences between MP-1 and MP-2 and between FC(B)-T and FC(B)-C were never higher than 0.5° . Such small values, in respect to the above reported MAV values, suggest that the sensor position and the subject position during FC(B) determine offsets between compared joint angles with negligible waveform distortions. In fact, contrary to MAV, WD has been defined to be not affected by offset between curves. Moreover, WD values for A_{IE} are not higher than the ones obtained for the other angles. This implies that a small misalignment between frontal planes of foot in FC(A) and FC(B) does not determine an important distortion of ankle angles during gait.

The analysis of the influence of different sensor positions and/or different subject positions in FC demonstrated that the calibration procedure here proposed can be considered robust in respect to the variability in sensor positioning, and in the subject position assumed in FC(B). Regardless, the highest differences among conditions were observable for ankle angles, demonstrating that the position of the foot during FC(B) represents the most delicate part of the FC procedure. This implies that subjects have to pay attention to avoid rotations of feet in frontal or transverse planes when they are performing the second phase of the FC procedure.

3.2. Test 2 – validation of FC in respect to a non-anatomical frame (O-TF_{MIMU} vs. O-TF_{OS})

Fig. 5 shows means and standard deviations of MAV (light gray bar) obtained comparing O-TF_{MIMU} and O-TF_{OS},

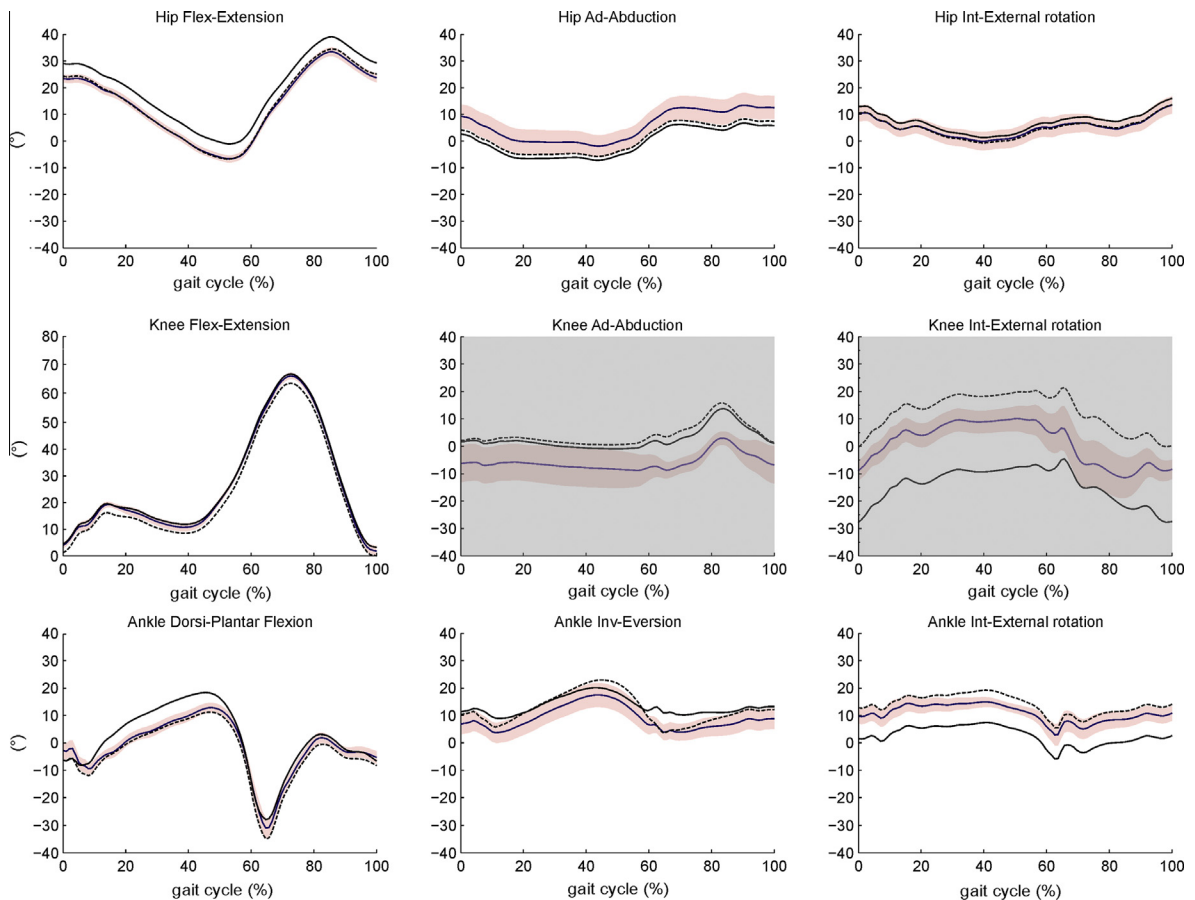


Fig. 4. Example of joint angular kinematics on one stride obtained from the three different output sets for subject 1 in MP-1 condition (right side). Six curves obtained from O-TF_{MIMU} are summarized by blue curve (mean) and pink stripe (\pm std). Black dashed curve was obtained from O-TF_{OS}, and black solid from O-ISB. Knee angles in frontal and transverse plane are grayed since they are not generally considered in clinical gait analysis. (For interpretation of the references to colour in this figure legend, the reader is referred to the web version of this article.)

Table 2

Mean (std) of mean absolute variability (MAV) values obtained in Test 1 reported in the different subject and sensor positions. Conditions statistically significant are marked.

Joint angle	Mean (std) MAV (°)							
	Left side				Right side			
	FC(B)-T		FC(B)-C		FC(B)-T		FC(B)-C	
	MP-1	MP-2	MP-1	MP-2	MP-1	MP-2	MP-1	MP-2
H _{FE}	2,9 (2,4)	2,3 (1,9)	2,9 (2,4)	2,3 (1,9)	3,0 (2,9)	3,3 (3,1)	3,1 (2,9)	3,2 (3,1)
H _{AA}	2,0 (1,8)	2,6 (2,0)	1,9 (1,6)	2,8 (2,0)	1,9 (1,2)	2,8 (2,0)	2,2 (1,3)	2,7 (1,8)
H _{IE}	3,9 (2,7)	2,5 (2,6)	2,8 (1,8)	2,3 (1,8)	3,3 (3,2)	3,0 (2,0)	3,1 (2,2)	3,7 (1,9)
K _{FE}	3,7 (2,4) [*]	1,3 (1,3) [†]	3,6 (2,4) [*]	1,3 (1,4) [†]	3,0 (2,7)	2,1 (1,7)	3,0 (2,7)	2,2 (1,7)
A _{DP}	3,1 (3,4)	2,3 (1,4)	3,2 (3,3)	2,1 (1,2)	3,4 (4,6)	1,7 (1,2)	2,6 (1,8)	1,7 (1,4)
A _{IV}	4,4 (2,9) [*]	2,2 (1,9) [†]	4,5 (2,7) [*]	2,5 (1,8) [†]	2,5 (2,0) [†]	3,9 (2,9) [*]	2,1 (1,5) [†]	4,0 (2,8) [*]
A _{IE}	11,5 (8,1)	9,7 (7,1)	8,9 (6,6)	8,2 (7,0)	10,2 (4,6) ^{**†}	6,5 (3,2) ^{**†}	9,5 (4,5) ^{**†}	4,7 (3,8) ^{**†}

^{*} Sensor position significant.

[†] Subject position significant.

averaging data among all the conditions in order to take into account the inter-subject variability of the FC(B) procedure, i.e. FC(B)-T and FC(B)-C, and the MIMU position (MP-1 and MP-2). Striped bars instead represent, for each angle, the reference values of MAV obtained with OS taking

into account the inter-variability of five different protocols typically adopted in gait analysis [39]. It is observable that the MAV value for each rotation comparing O-TF_{MIMU} and O-TF_{OS} is always lower than the reference ones. Thus, it is possible to state that uncertainty associated with the

Table 3

Mean (std) of waveform distortion (WD) values obtained in Test 1, reported in the different subject and sensor positions. Conditions statistically significant are marked.

Joint angle	Mean (std) WD (°)							
	Left side				Right side			
	FC(B)-T		FC(B)-C		FC(B)-T		FC(B)-C	
	MP-1	MP-2	MP-1	MP-2	MP-1	MP-2	MP-1	MP-2
H _{FE}	0,3 (0,3)	0,3 (0,2)	0,3 (0,2)	0,3 (0,2)	0,2 (0,1)	0,2 (0,1)	0,2 (0,2)	0,3 (0,1)
H _{AA}	0,6 (0,5)	0,7 (0,3)	0,6 (0,4)	0,7 (0,3)	0,6 (0,4)	0,7 (0,3)	0,6 (0,4)	0,6 (0,4)
H _{IE}	0,4 (0,2)	0,3 (0,2)	0,4 (0,1)	0,4 (0,2)	0,3 (0,2)	0,3 (0,2)	0,4 (0,2)	0,4 (0,2)
K _{FE}	0,4 (0,3) [*]	0,2 (0,1) [*]	0,3 (0,3) [*]	0,2 (0,1) [*]	0,2 (0,1)	0,5 (0,3)	0,2 (0,1)	0,5 (0,3)
A _{DP}	0,7 (0,4) ^{*†}	0,3 (0,1) ^{*†}	1,0 (0,5) ^{*†}	0,7 (0,3) ^{*†}	0,7 (0,3) [†]	0,3 (0,1) [*]	0,7 (0,3) [†]	0,3 (0,2) [*]
A _{IV}	0,8 (0,7) [†]	0,6 (0,2) [†]	1,3 (0,6) [†]	0,9 (0,5) [†]	0,9 (0,8) [†]	0,5 (0,3) [*]	0,8 (0,4) [†]	0,5 (0,3) [*]
A _{IE}	0,4 (0,2)	0,3 (0,2)	0,4 (0,1)	0,4 (0,2)	0,3 (0,2)	0,3 (0,2)	0,4 (0,2)	0,4 (0,2)

^{*} Sensor position significant.

[†] Subject position significant.

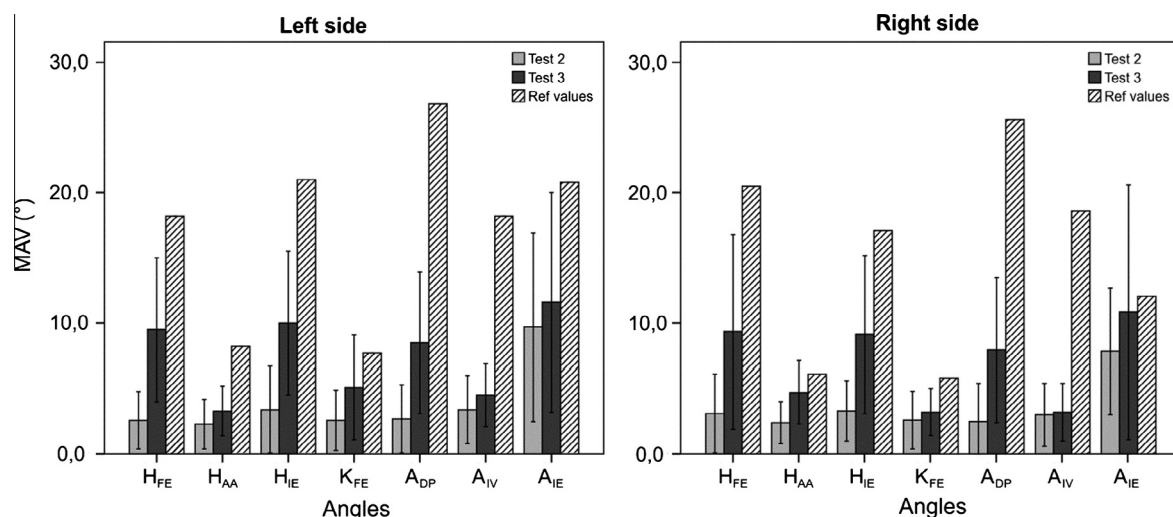


Fig. 5. Mean absolute variability (MAV) mean values (with \pm std error bar) computed in Test 2 (O-TF_{MIMU} vs. O-TF_{OS}) and Test 3 (O-TF_{MIMU} vs. O-ISB) for each joint angle. Reference value bars have been obtained from [39].

proposed calibration procedure can be considered comparable with the repeatability usually accepted in OS-based gait analysis, and due to the use of different protocols. The procedure showed accuracy and repeatability values less than 4° for each angle except for the ankle int-external rotation. In particular, the smallest value of accuracy (mean MAV) was observable for left H_{AA} (2.3°); the highest value for left A_{IE} (9.7°). The lowest value of repeatability (MAV std) was obtained for right H_{AA} (1.6°), the highest one for left A_{IE} (7.2°). These results confirm that a low accuracy of the FC procedure is due to the wrong orientation of the feet during FC(B).

Table 4 reports mean and standard deviation values of WD, expressed also as a percentage of the specific angle ROM. It is possible to observe that waveform distortions are never higher than 1° for each angle. The maximum value was obtained for left A_{IV} (4.1%), minimum values for left K_{FE} and right H_{FE} (0.5%). Left A_{IV} presented also the highest variability (2.7%). Lower values obtained for

WD, respect to MAV ones in Test 2, indicate that FC inaccuracy and unrepeatability are dominated by the offset between the reference curve obtained via OS and the FC repetitions curves.

It is worthy to remind that O-TF_{MIMU} was generated by the outputs of FC repetitions and the walking trial data both obtained via MIMU. Instead in O-TF_{OS} we merged the body-to-sensor calibration matrices obtained via OS, assumed as a reference, and the same walking trial data-set acquired by MIMU. Thus, the computed errors can be ascribed only to the inherent differences between the calibration procedures, and not to the worst metrological performances in 3D motion tracking of MIMU in respect to the OS.

Table 5 reports minimum values of the Pearson correlation coefficient. In Test 2 the correlation coefficients are between “very good” and “excellent”. These results confirm that the estimation of technical frame orientation with FC implies a small offset, without a noticeable distortion of joint angle waveforms.

Table 4

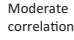


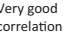
Mean (std) waveform distortion (WD) values expressed in degrees and as a percentage of the specific joint angular RoM, obtained in Test 2 and Test 3.

Joint angle	WD							
	Left				Right			
	Test 2		Test 3		Test 2		Test 3	
	(°)	(%)	(°)	(%)	(°)	(%)	(°)	(%)
H _{FE}	0.3 (0.2)	0.8 (0.5)	0.4 (0.2)	1.1 (0.5)	0.2 (0.1)	0.5 (0.3)	0.4 (0.3)	1.1 (0.8)
H _{AA}	0.6 (0.4)	3.5 (2.3)	0.9 (0.4)	5.3 (2.3)	0.6 (0.4)	3.5 (2.3)	0.8 (0.4)	4.7 (2.3)
H _{IE}	0.4 (0.2)	2.5 (1.3)	0.6 (0.4)	3.8 (2.5)	0.4 (0.2)	2.5 (1.3)	0.8 (0.5)	5.1 (3.2)
K _{FE}	0.3 (0.2)	0.5 (0.3)	0.6 (0.6)	0.9 (0.9)	0.4 (0.3)	0.6 (0.5)	0.6 (0.4)	0.9 (0.6)
A _{DP}	0.7 (0.4)	2.1 (1.2)	1.3 (0.8)	3.9 (2.4)	0.6 (0.3)	1.8 (0.9)	0.8 (0.4)	2.4 (1.2)
A _{IV}	0.9 (0.6)	4.1 (2.7)	1.9 (1.3)	8.6 (5.9)	0.7 (0.5)	3.2 (2.3)	1.1 (0.7)	5.0 (3.2)
A _{IE}	0.3 (0.2)	1.2 (0.8)	0.6 (0.3)	2.3 (1.2)	0.6 (0.5)	2.3 (1.9)	0.8 (0.5)	3.1 (1.9)

Table 5

Minimum values of Pearson correlation coefficient obtained in Test 2 and Test 3. Moderate correlation: r between 0.65 and 0.75; good correlation: r between 0.75 and 0.85; very good correlation: r between 0.85 and 0.95; excellent correlation: r between 0.95 and 1.

Joint angle	Minimum values of the Pearson correlation coefficient (r)			
	Left		Right	
	Test 2	Test 3	Test 2	Test 3
H _{FE}	0.951	0.950	0.989	0.978
H _{AA}	0.946	0.870	0.957	0.945
H _{IE}	0.968	0.963	0.896	0.945
K _{FE}	0.981	0.978	0.972	0.954
A _{DP}	0.922	0.841	0.921	0.894
A _{IV}	0.918	0.685	0.913	0.729
A _{IE}	0.968	0.963	0.896	0.945

Moderate correlation:  Good correlation:  Very good correlation:  Excellent correlation: 

3.3. Test 3 – validation of FC in respect to the standard anatomical frame ISB (O-TF_{MIMU} vs. O-ISB)

In Fig. 5 dark gray bars represent mean and standard deviation of MAV values obtained comparing O-TF_{MIMU} and O-ISB, similarly to Test 2. Accuracy values obtained with FC with respect to OS using JCS definition are always lower than the reference ones (striped bars). The smallest values were observable for K_{FE} and A_{IV} on the right side (3.2°); the highest value has been reported for left A_{IE} (11.6°). Considering repeatability, the lowest value was obtained for right K_{FE} (1.8°), the highest one for left A_{IE} (9.7°). Accuracy and repeatability reported for Test 3 are higher than in Test 2, which can be ascribed to inter-subject variability. In fact, relative rotations between TF and the standard JCS are subject-dependant. In the FC procedure the z -axis direction for body segments is defined as parallel to the vertical axis during the upright posture. Each subject, anyway, has a particular posture in the upright standing, with a different inclination of anatomical axes of each body segment with respect to the vertical axis. This entails the presence of an offset between TF and JCS defined by ISB, which is different for each subject. For this reason, the variability of the MAV index is definitely higher than the one evaluated in Test 2 (error bars in Fig. 5).

Mean and standard deviation values of WD, expressed also as a percentage of the specific angle ROM for the Test

3 are reported in Table 4. Mean WD values are always lower than 2°, and they are slightly greater than the corresponding ones in Test 2. The same trend is observable for the standard deviation of WD. The maximum value was obtained for left A_{IV} (8.6%), the minimum value for K_{FE} on both sides (0.6%). Similarly to Test 2, left A_{IV} also showed the highest variability (5.9%), and left H_{FE} the lowest (0.5%). These results suggest that the offset is the main component of uncertainty also with respect to standard JCS definition.

Table 5 reports minimum values of correlation coefficients obtained in Test 3. Most of the angles presented a high level of correlation (from good to excellent), with unnoticeable differences in respect to Test 2. Instead, decreases in r values are observable between Test 2 and Test 3 for: left A_{DP} (from very good to good); left A_{IV} (from very good to moderate); right H_{AA} (from excellent to very good); and, finally, right A_{IV} (from very good to moderate). That behaviour can be justified considering that a relevant offset, occurred in the estimation of TF with respect to standard JCS, affects the whole Cardan decomposition of the movement, entailing angle curves dissimilarity.

Hence, it is important to underscore that the main limitation of the here proposed calibration procedure resulted in the ability of the subject to maintain the sagittal plane, of each involved body segment, as parallel as possible during the two phases of the FC procedure, especially for the foot.

4. Conclusions

In this work we proposed a novel functional body-to-sensor calibration procedure for MIMU-based gait analysis. The procedure has been designed to be easy for the subject to perform autonomously. In fact, the calibration protocol needs neither a precise sensor positioning, nor the performance of specific and accurate movements.

The procedure produced robust results in respect to different sensor positions on the body, or different levels of subject inclination during the second static position. Procedure accuracy and repeatability have been found encouraging, both with respect to technical frame and the Joint Coordinate System definition evaluated by means of an optoelectronic system. In particular, the index for the mean absolute variability (MAV) value produced lower

results in both cases than the same index reported in the literature for a comparison among the five most-adopted protocols in OS-based gait analysis. The joint angle offset proved to be the main component of the inaccuracy related to the proposed functional procedure; waveform distortions (WD), instead, resulted negligible. Inter-subject repeatability increased in comparison to the standard JCS definition proposed by ISB, due to the specific body segment inclination of each subject in the upright position.

Acknowledgments

The authors would like to thank the **Italian Institute of Technology for the grant (2009) “Project Seed ITINERE – Interactive Technology: an Instrumented Novel Exoskeleton for Rehabilitation”** 2009 (Principal Investigator: P. CAPPÀ), and the Italian Health Ministry for the grant (2009) “Pilot study on a novel typology of medical devices: robotic exoskeletons for knee rehabilitation” (Principal Investigator: P. CAPPÀ).

References

- [1] E.R. Bachmann, X.P. Yun, R.B. McGhee, Sourceless tracking of human posture using small inertial/magnetic sensors, in: 2003 IEEE International Symposium on Computational Intelligence in Robotics and Automation, vol. I-ii, Proceedings, 2003, pp. 822–829.
- [2] D.T.P. Fong, Y.Y. Chan, The use of wearable inertial motion sensors in human lower limb biomechanics studies: a systematic review, *Sens.-Basel* 10 (2010) 11556–11565.
- [3] A.M. Sabatini, C. Martelloni, S. Scapellato, F. Cavallo, Assessment of walking features from foot inertial sensing, *IEEE T Bio-Med. Eng.* 52 (2005) 486–494.
- [4] C.M. Senanayake, S.M.N.A. Senanayake, Computational intelligent gait-phase detection system to identify pathological gait, *IEEE T Inf. Technol. B* 14 (2010) 1173–1179.
- [5] K.D. Nguyen, I.M. Chen, Z.Q. Luo, S.H. Yeo, H.B.L. Duh, A wearable sensing system for tracking and monitoring of functional arm movement, *IEEE-Asme T Mech.* 16 (2011) 213–220.
- [6] J. Liu, T.E. Lockhart, Automatic individual calibration in fall detection – an integrative ambulatory measurement framework, *Comput. Methods Biomech. Biomed. Eng.* 16 (2013) 504–510.
- [7] S. Kim, M.A. Nussbaum, Performance evaluation of a wearable inertial motion capture system for capturing physical exposures during manual material handling tasks, *Ergonomics* 56 (2013) 314–326.
- [8] T. Liu, Y. Inoue, K. Shibata, Development of a wearable sensor system for quantitative gait analysis, *Measurement* 42 (2009) 978–988.
- [9] N. Abaid, P. Cappa, E. Palermo, M. Petrarca, M. Porfiri, Gait detection in children with and without hemiplegia using single-axis wearable gyroscopes, *PLoS ONE* 8 (2013) e73152.
- [10] K. Parsa, T.A. Lasky, B. Ravani, Design and implementation of a mechatronic, all-accelerometer inertial measurement unit, *IEEE-Asme T Mech.* 12 (2007) 640–650.
- [11] P. Cappa, F. Patanè, S. Rossi, A redundant accelerometric cluster for the measurement of translational and angular acceleration and angular velocity of the head, *J. Med. Dev., Trans. ASME* 1 (2007) 14–22.
- [12] P. Cappa, F. Patanè, S. Rossi, Two calibration procedures for a gyroscope-free inertial measurement system based on a double-pendulum apparatus, *Meas. Sci. Technol.* 19 (2008).
- [13] K. Aminian, B. Najafi, Capturing human motion using body-fixed sensors: outdoor measurement and clinical applications, *Comput. Animat. Virt. W* 15 (2004) 79–94.
- [14] A.M. Sabatini, Adaptive filtering algorithms enhance the accuracy of low-cost inertial/magnetic sensing in pedestrian navigation systems, *Int. J. Comput. Intell. Appl.* 7 (2008) 351–361.
- [15] A.M. Sabatini, Quaternion-based extended Kalman filter for determining orientation by inertial and magnetic sensing, *IEEE T Bio-Med. Eng.* 53 (2006) 1346–1356.
- [16] D. Gebre-Egziabher, G.H. Elkaim, J.D. Powell, B.W. Parkinson, A non-linear, two-step estimation algorithm for calibrating solid-state strapdown magnetometers, in: *IEEE/AIAA (Ed.) 8th International St. Petersburg Conference on Navigation Systems*, St. Petersburg, Russia, 2001.
- [17] W.H.K. de Vries, H.E.J. Veeger, C.T.M. Baten, F.C.T. van der Helm, Magnetic distortion in motion labs, implications for validating inertial magnetic sensors, *Gait Posture* 29 (2009) 535–541.
- [18] C. Kendell, E.D. Lemaire, Effect of mobility devices on orientation sensors that contain magnetometers, *J. Rehabil. Res. Dev.* 46 (2009) 957–962.
- [19] D. Roetenberg, P.J. Slycke, P.H. Veltink, Ambulatory position and orientation tracking fusing magnetic and inertial sensing, *IEEE T Bio-Med. Eng.* 54 (2007) 883–890.
- [20] E. Palermo, S. Rossi, F. Patanè, P. Cappa, Experimental evaluation of indoor magnetic distortion effects on gait analysis performed with wearable inertial sensors, *Physiol. Meas.* 35 (2014) 399–415.
- [21] H. Wang, H. Lenz, A. Szabo, J. Bamberger, U.D. Hanebeck, WLAN-Based pedestrian tracking using particle filters and low-cost MEMS sensors, *WPNC'07: 4th workshop on positioning navigation and communication 2007*, Workshop Proc. (2007) 1–7.
- [22] E.H. Shin, N. El-Sheimy, An unscented Kalman filter for in-motion alignment of low-cost IMUs, *Plans 2004: Position Location and Navigation Symposium*, 2004, pp. 273–279.
- [23] M. St-Pierre, D. Gingras, Comparison between the unscented Kalman filter and the extended Kalman filter for the position estimation module of an integrated navigation information system, 2004, *IEEE Intelligent Vehicles Symp.* (2004) 831–835.
- [24] D. Roetenberg, H.J. Luinge, C.T.M. Baten, P.H. Veltink, Compensation of magnetic disturbances improves inertial and magnetic sensing of human body segment orientation, *IEEE T Neur. Syst. Reh.* 13 (2005) 395–405.
- [25] P. Picerno, A. Cereatti, A. Cappozzo, Joint kinematics estimate using wearable inertial and magnetic sensing modules, *Gait Posture* 28 (2008) 588–595.
- [26] H.J. Luinge, P.H. Veltink, C.T.M. Baten, Ambulatory measurement of arm orientation, *J. Biomech.* 40 (2007) 78–85.
- [27] A.G. Cutti, A. Giovanardi, L. Rocchi, A. Davalli, R. Sacchetti, Ambulatory measurement of shoulder and elbow kinematics through inertial and magnetic sensors, *Med. Biol. Eng. Comput.* 46 (2008) 169–178.
- [28] K.J. O'Donovan, R. Kamnik, D.T. O'Keeffe, G.M. Lyons, An inertial and magnetic sensor based technique for joint angle measurement, *J. Biomech.* 40 (2007) 2604–2611.
- [29] J. Favre, R. Aissaoui, B.M. Jolles, J.A. de Guise, K. Aminian, Functional calibration procedure for 3D knee joint angle description using inertial sensors, *J. Biomech.* 42 (2009) 2330–2335.
- [30] A.G. Cutti, A. Ferrari, P. Garofalo, M. Raggi, A. Cappello, A. Ferrari, “Outwalk”: a protocol for clinical gait analysis based on inertial and magnetic sensors, *Med. Biol. Eng. Comput.* 48 (2010) 17–25.
- [31] A. Ferrari, A.G. Cutti, P. Garofalo, M. Raggi, M. Heijboer, A. Cappello, A. Davalli, First in vivo assessment of “Outwalk”: a novel protocol for clinical gait analysis based on inertial and magnetic sensors, *Med. Biol. Eng. Comput.* 48 (2010) 1–15.
- [32] G. Uswatte, E. Taub, D. Morris, M. Vignolo, K. McCulloch, Reliability and validity of the upper-extremity motor activity Log-14 for measuring real-world arm use, *Stroke* 36 (2005) 2493–2496.
- [33] A. Salarian, H. Russmann, F.J.G. Vingerhoets, C. Dehollain, Y. Blanc, P.R. Burkhard, K. Aminian, Gait assessment in Parkinson's disease: toward an ambulatory system for long-term monitoring, *IEEE T Bio-Med. Eng.* 51 (2004) 1434–1443.
- [34] S.T. Moore, H.G. MacDougall, J.M. Gracies, H.S. Cohen, W.G. Ondo, Long-term monitoring of gait in Parkinson's disease, *Gait Posture* 26 (2007) 200–207.
- [35] P. Picerno, A. Cereatti, A. Cappozzo, A spot check for assessing static orientation consistency of inertial and magnetic sensing units, *Gait Posture* 33 (2011) 373–378.
- [36] G. Wu, S. Siegler, P. Allard, C. Kirtley, A. Leardini, D. Rosenbaum, M. Whittle, D.D. D'Lima, L. Cristofolini, H. Witte, O. Schmid, H. Stokes, ISB recommendation on definitions of joint coordinate system of various joints for the reporting of human joint motion – part 1: ankle, hip, and spine, *J. Biomech.* 35 (2002) 543–548.
- [37] R.B. Davis, S. Ounpuu, D. Tyburski, J.R. Gage, A gait analysis data-collection and reduction technique, *Human Movement Sci.* 10 (1991) 575–587.
- [38] D.K. Ramsey, P.F. Wretenberg, Biomechanics of the knee: methodological considerations in the in vivo kinematic analysis of the tibiofemoral and patellofemoral joint, *Clin. Biomech.* 14 (1999) 595–611.
- [39] A. Ferrari, M.G. Benedetti, E. Pavan, C. Frigo, D. Bettinelli, M. Rabuffetti, P. Crenna, A. Leardini, Quantitative comparison of five current protocols in gait analysis, *Gait Posture* 28 (2008) 207–216.